Archives of Toxicology
https://doi.org/10.1007/s00204-018-2202-3

GENOTOXICITY AND CARCINOGENICITY

Loss of Wilms tumor 1 protein is a marker for apoptosis in response to replicative stress in leukemic cells

Miriam Pons[1] · Claudia M. Reichardt[2] · Dorle Hennig[3,9] · Abinaya Nathan[2] · Nicole Kiweler[1] · Carol Stocking[4] · Christian Wichmann[5] · Markus Christmann[1] · Falk Butter[6] · Sigrid Reichardt[3] · Günter Schneider[7] · Thorsten Heinzel[3] · Christoph Englert[2,3] · Jörg Hartkamp[8] · Oliver H. Krämer[1] · Nisintha Mahendrarajah[1]

Received: 16 March 2018 / Accepted: 22 March 2018

Abstract

A remaining expression of the transcription factor Wilms tumor 1 (WT1) after cytotoxic chemotherapy indicates remaining leukemic clones in patients. We determined the regulation and relevance of WT1 in leukemic cells exposed to replicative stress and DNA damage. To induce these conditions, we used the clinically relevant chemotherapeutics hydroxyurea and doxorubicin. We additionally treated cells with the pro-apoptotic kinase inhibitor staurosporine. Our data show that these agents promote apoptosis to a variable extent in a panel of 12 leukemic cell lines and that caspases cleave WT1 during apoptosis. A chemical inhibition of caspases as well as an overexpression of mitochondrial, anti-apoptotic BCL2 family proteins significantly reduces the processing of WT1 and cell death in hydroxyurea-sensitive acute promyelocytic leukemia cells. Although the reduction of WT1 correlates with the pharmacological efficiency of chemotherapeutics in various leukemic cells, the elimination of WT1 by different strategies of RNA interference (RNAi) does not lead to changes in the cell cycle of chronic myeloid leukemia K562 cells. RNAi against WT1 does also not increase the extent of apoptosis and the accumulation of γH2AX in K562 cells exposed to hydroxyurea. Likewise, a targeted genetic depletion of WT1 in primary oviduct cells does not increase the levels of γH2AX. Our findings position WT1 as a downstream target of the apoptotic process that occurs in response to cytotoxic forms of replicative stress and DNA damage.

Keywords Apoptosis · DNA damage · Caspase · Hydroxyurea · Leukemia · Replicative stress · WT1

Introduction

The WT1 protein contains an N-terminal transcriptional regulatory domain and four C-terminal Krüppel-type zinc fingers (Ariyaratana and Loeb 2007; Hastie 2017; Huff 2011;

Miriam Pons and Claudia M. Reichardt: equal first author contribution. Jörg Hartkamp, Oliver H. Krämer and Nisintha Mahendrarajah: equal last author contribution.

Electronic supplementary material The online version of this article (https://doi.org/10.1007/s00204-018-2202-3) contains supplementary material, which is available to authorized users.

✉ Oliver H. Krämer
okraemer@uni-mainz.de

1 Department of Toxicology, University Medical Center, Obere Zahlbacher Str. 67, 55131 Mainz, Germany

2 Molecular Genetics, Leibniz Institute for Age Research, Fritz-Lipmann-Institute, Beutenberg Str. 11, 07745 Jena, Germany

3 Department of Biochemistry, Institute of Biochemistry and Biophysics, Center for Molecular Biomedicine, Friedrich-Schiller-University Jena, Hans-Knöll-Straße 2, 07745 Jena, Germany

4 Heinrich Pette Institute, Leibniz Institute for Experimental Virology, Hamburg, Germany

5 Department of Transfusion Medicine, Cell Therapeutics and Hemostaseology, Ludwig-Maximilian University Hospital, Munich, Germany

6 Institute of Molecular Biology (IMB), Mainz, Germany

7 Klinik und Poliklinik für Innere Medizin II, Technical University of Munich, 81675 Munich, Germany

8 Institute of Biochemistry and Molecular Biology, Medical School, RWTH Aachen University, Aachen, Germany

9 Present Address: Department of Molecular Medicine, University of Southern Denmark, J. B. Winsløws Vej 25, 5000 Odense, Denmark

Published online: 27 March 2018

Rampal and Figueroa 2016). Four major WT1 isoforms are generated by two alternative splicing events. Whereas exon 5 isoforms include or exclude 17 amino acids (17AA) between the transcriptional regulatory domain and the zinc finger domain, the second splicing event inserts three amino acids [lysine–threonine–serine (KTS)] between zinc fingers three and four. The isoforms lacking the KTS insertions (− KTS) bind DNA with high affinity and function as transcriptional regulators, whereas splice variants including the KTS insertion (+ KTS) have a lower affinity for DNA and also act via posttranscriptional processes (Ariyaratana and Loeb 2007; Hastie 2017; Huff 2011; Rampal and Figueroa 2016).

Several studies report an increased expression of WT1 in CML, acute myeloid leukemia (AML), acute lymphoblastic leukemia, and myelodysplastic syndrome (Ariyaratana and Loeb 2007; Hastie 2017; Huff 2011; Rampal and Figueroa 2016). Moreover, remaining *WT1* mRNA levels in the bone marrow or peripheral blood after cytotoxic chemotherapy indicate minimal residual disease (Ariyaratana and Loeb 2007; Gray et al. 2012; Grimwade et al. 2010; Kühnl et al. 2011; Lapillonne et al. 2006; Varma et al. 2011). Moreover, a loss of WT1 shows the success of AML therapy with cytarabine/idarubicin (Gianfaldoni et al. 2010). However, while leukemic stem cells have higher levels of WT1 than normal hematopoietic stem cells, an overexpression of WT1 does not promote an oncogenic accumulation of hematopoietic stem and progenitor cells (Hosen et al. 2007). Furthermore, a subtype of leukemic cells carries loss-of-function mutations in WT1, which can be linked to chemoresistance (Ariyaratana and Loeb 2007; Hastie 2017; Huff 2011; Rampal and Figueroa 2016). Conflicting data also exist regarding the use of WT1 as a prognostic factor. While earlier reports show that high levels of WT1 correlate with poor prognosis in AML patients (Bergmann et al. 1997), recent data demonstrate that high WT1 levels before therapy correlate with increased leukemia-free survival of AML patients treated with arabinofuranosylcytidine (Miglino et al. 2011). Obviously, there is the need for a more thorough characterization of the functions of WT1 in leukemic cells.

In order to define a putative role of WT1 for the success of anti-leukemic chemotherapy, it is necessary to understand the pathways that chemotherapy triggers. Most chemotherapeutic drugs induce replicative stress and DNA damage which cause apoptosis and other cell death modes (Dobbelstein and Sørensen 2015). Apoptosis involves the enzymatic dismantling of cells by caspases (Czabotar et al. 2014; Fulda 2015). Mitochondrial anti- and pro-apoptotic BCL2 proteins regulate apoptosis via a stabilization or destabilization of mitochondrial membranes, respectively (Czabotar et al. 2014; Fulda 2015). Anti-apoptotic BCL2 proteins, e.g., BCL-XL, BCL2, MCL1, and A1/BFL1 prevent and pro-apoptotic BCL2 proteins BAX and BAK promote the initiation and formation of mitochondrial pores (Loeb 2006; Ni Chonghaile and Letai 2008). Such pores allow the efflux of cytochrome c, which activates the initiator caspase-9 in a complex with the apoptosis-activating factor APAF-1 (Czabotar et al. 2014; Loeb 2006; Ni Chonghaile and Letai 2008). Caspase-9 subsequently activates the main apoptosis executioner enzyme caspase-3 (Czabotar et al. 2014). Apart from this intrinsic pathway of apoptosis induction, cells can undergo the extrinsic apoptosis pathway, which is mediated by death receptors, caspase-8, and a subsequent activation of caspase-3 (Fulda 2015). Caspase-8 and -9 themselves also degrade cellular proteins and additional members of the caspase family regulate apoptosis as well as inflammatory responses (Czabotar et al. 2014; Fulda 2015; Loeb 2006; Ni Chonghaile and Letai 2008).

It has been reported that WT1 promotes the expression of anti-apoptotic genes and represses pro-apoptotic genes in leukemic cells. Examples are BCL-XL (Bansal et al. 2012), BCL2 and the transcription factor c-MYC (Bansal et al. 2010; Ruan et al. 2018), A1/BFL1 (Simpson et al. 2006), survival signaling via MAP and JAK kinases (Li et al. 2014), BAX and BAX (Ito et al. 2006), and ZNF224 (Montano et al. 2013, 2015). However, WT1 has also been found to enhance the levels of the death receptor CD95L, which triggers apoptosis in T-cell leukemia cells (Bourkoula et al. 2014). Moreover, WT1 transcriptionally activates the expression of the tumor-suppressive long non-coding RNA *maternally-expressed-gene-3*. This effect relies on WT1's interaction with the ten-eleven-translocation-2 (TET2) enzyme, which promotes DNA demethylation (Lyu et al. 2017). The association between WT1 and TET2 and the resulting WT1-dependent regulation of genes reduces leukemic cell growth and this interaction between WT1 and TET2 is compromised in patient-associated WT1 mutants (Rampal et al. 2014; Wang et al. 2015). An induction of growth arrest and differentiation in human AML cells with overexpressed WT1 likewise suggests a tumor-suppressive role of WT1 (Ellisen et al. 2001). Due to such contrary data and owing to species- and tissue-specific functions of WT1, it is difficult to judge WT1 as a tumor suppressor or promoter (Hartkamp et al. 2010; Hastie 2017; Huff 2011; Rampal and Figueroa 2016).

The situation even becomes more complex as WT1 is a downstream target of the apoptosis machinery. In response to chemotherapeutic drugs, the serine protease HTRA2 (Hartkamp et al. 2010), and the apoptosis executioner caspase-3 (Ruan et al. 2018), cleave WT1 in solid and hematopoietic tumor cells. Furthermore, the E2 ubiquitin conjugase UBCH8 promotes the proteasomal degradation of WT1 in response to an inhibition of epigenetic modifiers of the histone deacetylase family (Makki et al. 2008). The biological relevance of these cleavage events and the proteasomal degradation of WT1 remains to be clarified.

Hydroxyurea is a standard drug against leukemia (Itzykson et al. 2013; Madaan et al. 2012). This drug inhibits ribonucleotide reductase, which synthesizes dNTPs. Consequently, cells arrest in G1/S phase and DNA breaks occur when stalled replication forks collapse (Dobbelstein and Sørensen 2015; Nikolova et al. 2017; Schlacher et al. 2011; Toledo et al. 2013). The homologous recombination (HR) pathway repairs such DNA lesions (Dobbelstein and Sørensen 2015; Nikolova et al. 2017; Schlacher et al. 2011; Toledo et al. 2013). Despite its frequent use against leukemic cells, it is unclear if hydroxyurea modulates WT1. Therefore, we asked whether hydroxyurea has an impact on WT1 and if WT1 affects the sensitivity of leukemic cells to replicative stress and DNA damage induced by hydroxyurea. To answer these questions, we additionally applied the DNA-damaging drug doxorubicin, which intercalates into DNA/RNA and blocks the DNA unwinding enzyme topoisomerase-II (Cruet-Hennequart et al. 2012), and the pro-apoptotic molecule staurosporine (Mahendrarajah et al. 2016).

We reveal that the stability of WT1 correlates with the induction of apoptosis and DNA damage in drug-exposed leukemic cells. Moreover, we confirm a caspase-dependent processing of WT1 in cells exposed to replicative stress and DNA damage. Strikingly, an inactivation of WT1 through RNA interference with transient siRNA transfection or stably expressed shRNA molecules does not affect cell cycle progression, apoptosis, or DNA damage in resting and stressed cells. This finding is supported by data obtained with leukemic cells devoid of WT1 and with genetically engineered oviduct cells with the possibility to eliminate WT1. Thus, WT1 is a biological target of caspases and a pharmacological marker for drug efficacy.

Materials and methods

Propagation of leukemic cells

Human leukemic cells (see Supplementary Table S1 for details) were cultured in RPMI medium supplemented with 10% FCS, 1% penicillin/streptomycin and 2% glutamine. NB4, K562, and MV4–11 cells were verified by DNA fingerprint at DSMZ, Braunschweig.

Primary oviduct cell culture and conditional knockout mice

Mice carrying conditional *Wt1* alleles ($Wt1^{fl/fl}$) were bred and maintained in the Animal Facility of the Leibniz Institute on Aging—Fritz Lipmann Institute (FLI), Jena, Germany, according to the rules of the German Animal Welfare Law. Animals were housed under specific pathogen-free conditions (SPF1), maintained on a 12-h light/dark cycle and were fed with mouse chow and tap water ad libitum. Oviducts from mice were dissected, washed in PBS and minced in a solution containing 50 µl of Collagenase A (10 ng/µl), 50 µl of DNase I (10 ng/µl) in 500 µl sterile PBS for 1 h at 37 °C at 800 rpm. The digested tissue was passed through a 70 µm cell strainer (BD-Biosciences) with the help of a piston of a syringe. The flow through was centrifuged and the cell pellet washed twice. Up to 3×10^5 cells could be obtained from two oviducts. After washing, the cell pellet was suspended in pre-warmed cell culture medium [DMEM F12 (Gibco) + 2% FCS, ZellShield (Minerva biolabs) and Reno supplement (Promocell)] and transferred onto gelatin-coated 12-well plates. Cells were left undisturbed for 72 h to allow cell attachment at 37 °C, 5% CO_2 and 95% humidity, followed by medium change. The attached cells appeared to be flat and spread out with tousled membranes resembling primary ampullary cells in culture (Bongso et al. 1989). Polygonal and elongated cells were also observed. The ciliary beating of epithelial cells was observed for up to 3 days in cultured dishes. In case of cells isolated from conditional knockout mice, the cells were treated after 72 h in culture with 2 µM 4′-OH tamoxifen for 72 h at 37 °C, 5% CO_2 and 95% humidity, to allow *Cre*-mediated recombination. Wildtype controls were treated with 2 µM 4′-OH tamoxifen at the same conditions. Cells were further propagated and maintained until seven divisions in vitro. Further details can be found in Supplementary Table S2.

Inhibitors and drugs

Staurosporine was from Selleck Chemicals; z-VAD-FMK was from Bachem; hydroxyurea and doxorubicin were from Sigma-Aldrich.

Lysate preparations, immunoblot and antibodies

Generation of cell extracts and immunoblot techniques were performed as described in (Beyer et al. 2017; Buchwald et al. 2010). The following antibodies were used (sources mentioned in brackets after the antibodies): BAK/ab32371, BAX/ab32503, p-RPA (T21)/ab61065, RAD51/ab63801, α-Tubulin/ab176560, WT1/ab201948 (Abcam); BCL-XL/51-6646GR, cleaved PARP1 (D214)/552596, PARP1/556362 (BD Pharmingen); p-CHK1 (S317)/A300-163A (Bethyl Laboratories, Inc); BCL-XL/bs-1336R and Vinculin/BZL-03106 (Biozol); cleaved Caspase-3 (D175)/9664, p-CHK1 (S317)/2344, CHK1/2360, p-CHK2 (T68)/2661, CHK2/2662, γH2AX/9718, p38/9212 (Cell Signaling); LDH (Chemicon International Inc./Merck Millipore); RPA/NA19L (Merck Millipore); WT1 (clone 6F-H2)/M3561 (Dako); HSP90/ADI-SPA-830-F (Enzo Life Sciences); p-ATR (T1989)/GTX128145 (GeneTex Inc); β-Actin/sc-47778, BAX/sc-20067, BCL-2/sc-492,

Caspase-3/sc-7272, GAPDH/sc-137179, HSP90/sc-13119, WT1/sc-192 (Santa Cruz Biotechnology); β-Actin/A2066, α-Tubulin/T5168 (Sigma-Aldrich).

Cell cycle analysis by propidium iodide staining of fixed cells

Cells were fixed with 70% ethanol at − 20 °C for at least 2 h and stained with propidium iodide (PI) staining solution (38 mM sodium citrate, 0.1 g/l propidium iodide, 0.1 g/l RNase A) for 20 min at 37 °C. Cells were analyzed with a FACS Canto flow cytometer (Becton Dickinson) or a FACS Canto II flow cytometer (BD-Biosciences).

Annexin V/PI staining of apoptotic cells

Staining was conducted according to the manufacturer's instructions with Annexin V-FITC (Becton Dickinson) and PI at RT for 15 min in the dark. Cells were analyzed with the FACS Canto flow cytometer (Becton Dickinson) or a FACS Canto II flow cytometer (BD-Biosciences). Early apoptotic cells are Annexin V-positive and PI-negative; late apoptotic or necrotic cells are Annexin V-positive and PI-positive.

DiOC staining for analysis of mitochondrial membrane potential (ψm)

3,3′-Dihexyloxacarbocyanine iodide [$DiOC_6(3)$] (Molecular Probes, Eugene) is a lipophilic, cationic, fluorescent dye used to monitor ψm in living cells. The dye detects changes in ψm ($\Delta\psi m$) by accumulating in the mitochondrial matrix. For staining, cells were incubated with 50 nM $DiOC_6$ for 30 min at 37 °C in the dark. Afterwards, cells were transferred into the flow cytometry tubes and centrifuged for 5 min at 700*g*. The supernatant was discarded and the cells were washed once in PBS to remove remaining medium and dye from the cell surface. Subsequently, the cell pellets were resuspended in 0.5 ml PBS and immediately measured on a FACS Canto II flow cytometer (BD-Biosciences) using the FITC-channel.

Immunofluorescence analyses

Coverslip preparation

20 × 20 mm coverslips were soaked for 20 min in diethyl ether and rinsed in a series of 100% ethanol, 70% ethanol, and ddH_2O. Then they were washed in 1 M HCl on a shaker for 20 min and rinsed in ddH_2O. Coverslips were stored in 70% ethanol until usage.

Cell culture

For the RPA/γH2AX immunofluorescence experiment the coverslips were placed in six-well plates. After the ethanol on the coverslips was evaporated, 3×10^5 leukemic cells were centrifuged at 317×*g* for 5 min and resuspended in 10 µl PBS. The cell suspension was dropped onto the coverslips and spread out with the tip. Proper cell density was verified with a light microscope. Cells were allowed to dry for 3–5 min at RT.

Fixation/blocking

The cells on the coverslips were fixed in 2 ml ice-cold methanol:acetone (7:3) per well for 6 min at − 20 °C, washed once with PBS, and fixed again for 10 min with 2.5% paraformaldehyde (PFA) at RT. After two additional washing steps with PBS, cells were blocked with 10% normal goat serum (Life Technologies)/PBS/0.1% Triton X-100 for 1 h at room temperature (RT).

Staining

The blocking solution was removed. Cells were incubated overnight at 4 °C with 100 µl primary antibody solution [RPA (Merck Millipore/NA19L) and γH2AX (Cell Signaling/9718)] diluted 1:1000 in 1% BSA/0.01% Triton/PBS. Then the coverslips were washed with PBS for 5 min, washed with PBS high salt (PBS + 0.4 M NaCl) for 2 min, and washed again with PBS for 5 min. All following steps were performed in the dark. Cells on the coverslips were incubated for 1 h at RT with 100 µl secondary antibody solution [F(ab)2 fragment AlexaFluor 488-conjugated goat anti-mouse (Life Technologies) and Cy3-conjugated goat anti-rabbit (Dianova/Jackson Immuno Research)] diluted 1:300 in 1% BSA/0.01% Triton/PBS. Coverslips were washed as described above for primary antibody. For nuclear staining, 100 µl To-Pro3 solution (100 µM stock solution, diluted 1:100 in PBS; Life Technologies) was added to the cells for 15 min. Meanwhile, glass slides were prepared by cleaning them with 70% ethanol and dropping 10 µl Vectashield mounting medium (Vector Laboratories) onto each slide. Coverslips containing the stained cells were dipped into PBS, turned upside down and placed onto glass slides coated with Vectashield. They were sealed with colourless nail polish to fix them on the slides. Slides were stored in the dark at 4 °C until analysis on the laser-scanning microscope LSM710 with Zen 2009 software (Carl Zeiss). Scoring of RPA foci on captured images was carried out with ImageJ software using an appropriate macro (50–100 cells/sample). The mean fluorescence intensity of γH2AX was quantified with imageJ.

Oviduct cells were grown on coverslips coated with poly-L-lysine (Sigma) for at least 48 h before staining. Monolayers on coverslips were washed thrice with PBS, fixed in 4% PFA for 30 min at RT and permeabilized with 0.3% Triton X-100/PBS for 10 min at RT. After washing with PBS, the coverslips were blocked with 2% BSA/5% FCS for 1 h at RT, followed by an incubation with primary antibodies (1:50) overnight at 4 °C. After washing with PBS, cells were treated with Alexa Fluor® secondary antibodies (1:1000) for 1 h at RT in the dark. After further washes, the coverslips were mounted on slides sealed with Prolong® Gold AntiFade reagent with DAPI (Life Technologies). Cells were analyzed and imaged with a Axio Apotome 2 microscope and the corresponding AxioVision software (Carl Zeiss).

Quantitative real-time PCR

Quantitative real-time PCR (qPCR) analysis was carried out in a 96-well-format on a Biorad iCycler using SYBR Green I (Sigma) for detection and Fluorescein (FITC; Biorad) for calibration. Composition of the master mix is given in Supplementary Table S3. Predilutions of the cDNA samples were 1:40 and of the 10,000× SYBR Green I stock 1:2000. Samples were measured in triplicates and normalized to *ACTB* (*β-Actin*), *GAPDH* (*Glycerinaldehyde-3-phosphate dehydrogenase*), *HPRT* (*Hypoxanthine guanine phosphoribosyl transferase*) and *TBP* (*TATA-box binding protein*). Data were analyzed using the iQ5 program and the relative expression software tool (Pfaffl et al. 2002). Oligonucleotides used in this study are stated in Supplementary Table S4.

Transduction of NB4 cells

Cells were retrovirally transduced with the vector constructs MSCV, MSCV-BCL2, or MSCV-BCL-XL, which all co-express EGFP (bicistronic vector). To increase transduction rates, retroviral particles were preloaded on retronectin. EGFP-positive, transduced cells were enriched by sorting using a FACS Aria cell sorter (BD-Biosciences, Heidelberg, Germany).

RNA interference

1×10^6 K562 cells were electroporated according to the protocol for K562 cells [ATCC®] with the Amaxa® Cell Line Nucleofector® Kit V (Lonza)/Ingenio kit solution (Mirus; 100 µl solution per sample). 100 pmol siRNA (non-targeting control siRNA-B/sc-44230 or siRNA targeting WT1/sc-36846) were applied for electroporation with the Amaxa® Nucleofector® II Device (Lonza) using program T-016. Cells were incubated for 24 h in 6 well plates with 2 ml fresh medium per well and reseeded into 12-well plates (without any washing steps in between). Following an equilibration time of 2 h, cells received drugs for 24–48 h.

To achieve stable WT1 knockdowns, the following plasmids from the Sigma-Aldrich Mission lentiviral shRNA library were used: WT1 (TRCN0000040063) and non-silencing control (SHC202). Lentiviral transduction procedures were carried out as described before (Treude et al. 2014); 1 µg/ml puromycin was added to lentivirally transduced K562 cells.

Raw data, uncropped western blots and immunofluorescence images shown in Fig. 1-S2 can be found in Supplementary Materials 1 and 2.

Results

Correlation between the stability of WT1 and the survival of leukemic cells exposed to replicative stress

We analyzed the responses of various leukemic cells to hydroxyurea. The exposure of Annexin V on the plasma membrane is a typical feature of apoptotic cells and can be measured by flow cytometry (Marx-Blümel et al. 2017). Using this method, we found that NB4 APL cells were very sensitive and that K562 CML cells were largely resistant to apoptosis induction by a 24 h exposure to 0.5 mM hydroxyurea (Fig. 1a).

Analyzing cell cycle profiles by flow cytometry, we noted that K562 cells arrested in G1/S phase in response to hydroxyurea. NB4 cells succumbed to cell death and lost most S and G2/M phase cells (Fig. 1b). Analyzing the percentage of cells in the subG1 phase, i.e., cells with DNA contents below 2N due to apoptotic chromatin fragmentation (Marx-Blümel et al. 2017), we could confirm that NB4 cells undergo cell death in response to hydroxyurea (Fig. 1b, Supplementary Fig. S1a).

To further verify that a 24 h exposure to 0.5 mM hydroxyurea triggers apoptosis in NB4 cells, we tested for typical apoptosis markers. These include the proteolysis-dependent activation of caspase-3 and the cleavage of its substrate PARP1 (Marx-Blümel et al. 2017). Hydroxyurea-treated NB4 cells showed both apoptosis markers and K562 cells none of them (Fig. 1c).

Since it has not been clarified whether hydroxyurea affects the expression of WT1 in leukemic cells and if this is linked to their sensitivity, we treated a panel of leukemic cells with hydroxyurea. We then analyzed lysates from these cells by immunoblot. After a 24 h exposure time to hydroxyurea, some leukemic cells had reduced WT1 levels (NB4, MV4-11, HEL, and BV-173 cells), while WT1 remained present in K562, KCL-22,

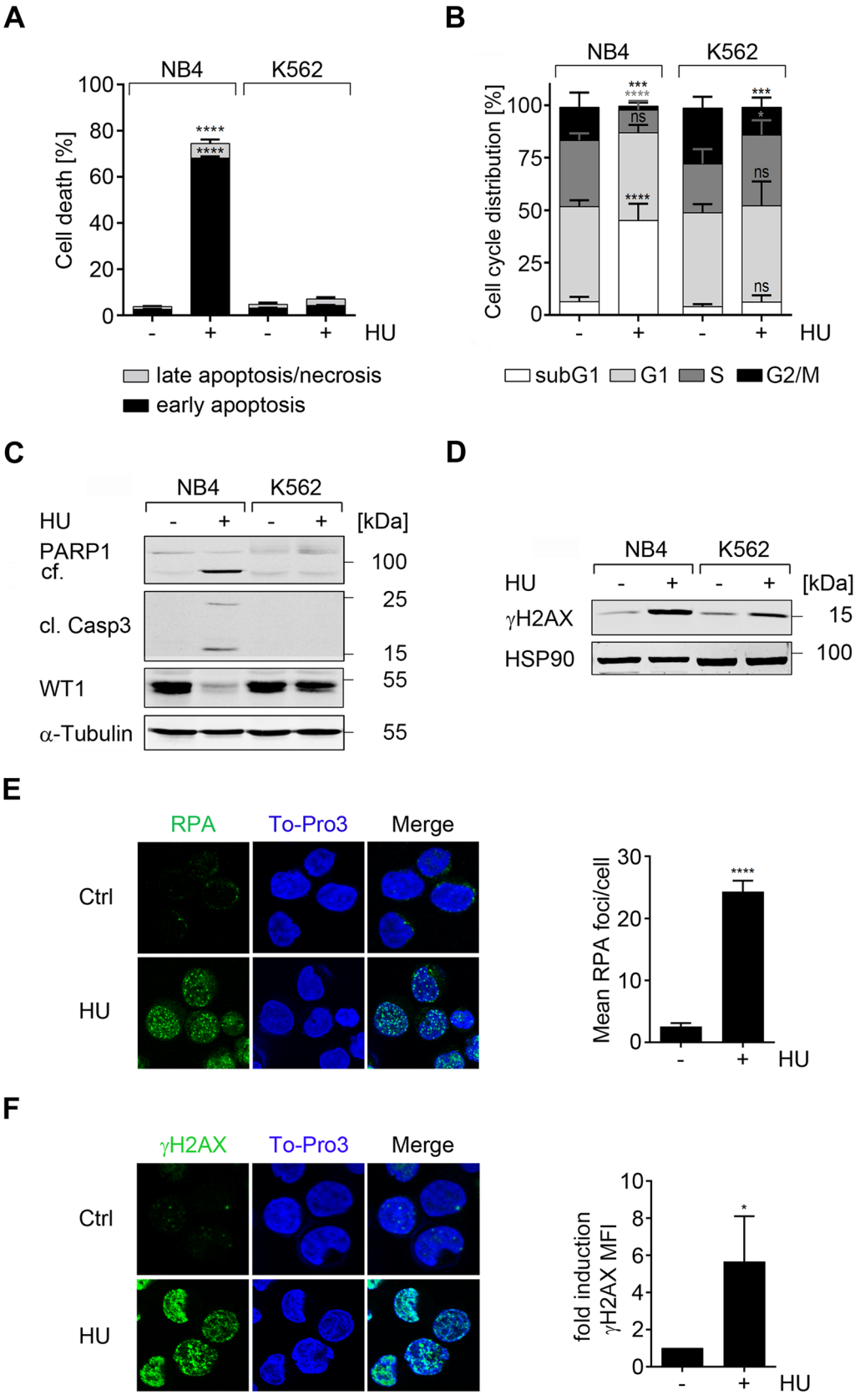
A
NB4
K562
Cell death [%]
100
80
60
40
20
0
****
****
- + - +
HU
late apoptosis/necrosis
early apoptosis
B
NB4
K562
Cell cycle distribution [%]
100
75
50
25
0
***
****
ns
****
***
*
ns
ns
- + - +
HU
subG1
G1
S
G2/M
C
NB4
K562
HU
- + - +
[kDa]
PARP1 cf.
100
cl. Casp3
25
15
WT1
55
α-Tubulin
55
D
NB4
K562
HU
- + - +
[kDa]
γH2AX
15
HSP90
100
E
RPA
To-Pro3
Merge
Ctrl
HU
Mean RPA foci/cell
30
20
10
0
****
- + HU
F
γH2AX
To-Pro3
Merge
Ctrl
HU
fold induction γH2AX MFI
10
8
6
4
2
0
*
- + HU

◂**Fig. 1** Stability of WT1 in leukemic cells exposed to replicative stress correlates with survival. **a** NB4 and K562 cells were treated with 0.5 mM hydroxyurea (HU) for 24 h. For cell death analysis, Annexin V/PI-stained cells were measured by flow cytometry; $n = 3 \pm$ SD; two-way ANOVA; Bonferroni's multiple comparisons test; $^{****}p < 0.0001$. **b** Cells treated with 0.5 mM HU for 24 h were analyzed for cell cycle distributions via flow cytometry assessing DNA contents of fixed and PI-treated cells; $n = 3 \pm$ SD; two-way ANOVA; Bonferroni's multiple comparisons test; $^{*}p < 0{,}05$, $^{***}p < 0.001$, $^{****}p < 0.0001$, *ns* not significant. **c** Analysis of PARP1, cleaved caspase-3 (cl. Casp3), and WT1, by immunoblot; α-Tubulin, loading control; cf., cleaved fragment. K562 and NB4 cells were incubated with 0.5 mM HU for 24 h. **d** Immunoblot of γH2AX; HSP90, loading control; cells were treated as stated in **c. e** RPA staining (green) of K562 cells exposed to 1 mM HU for 24 h. To-Pro3 (blue) was used for nuclear staining. Representative confocal images and the quantification of RPA foci are shown; $n = 3 \pm$ SD; unpaired, two-tailed Student's *t* test; $^{****}p < 0.0001$. **f** Immunofluorescence shows γH2AX stained K562 cells (green) treated with 1 mM HU for 24 h. To-Pro3 (blue) was used for nuclear staining. Representative confocal images and the quantification of γH2AX mean fluorescence intensity (MFI) are shown; $n = 3 \pm$ SD; unpaired, two-tailed Student's *t* test; $p = 0.0301$. (Color figure online)

and KYO-01 cells (Fig. 1c, Supplementary Fig. S1b-c). All cell cultures in which hydroxyurea lessened WT1 expression showed increased cell death (Fig. 1a, b, Supplementary Fig. S1b). Those cells that kept stable levels of WT1 did not show increased levels of cell death although hydroxyurea altered the proportions of cells in the S and G2/M phases significantly (Fig. 1a, b, Supplementary Fig. S1d). These experiments show that a loss of WT1 indicates cellular sensitivity to hydroxyurea.

Next, we asked if this differential sensitivity of leukemic cells to hydroxyurea ties in with different amounts of replicative stress and DNA damage. By Western blot, we tested for phosphorylated histone H2AX at residue S139 (γH2AX), which accumulates when replication forks are obstructed and when DNA becomes damaged (Dobbelstein and Sørensen 2015; Nikolova et al. 2017; Rogakou et al. 1998; Schlacher et al. 2011; Toledo et al. 2013). We found that the more hydroxyurea-sensitive NB4 cell line accumulated more γH2AX than the less sensitive K562 cell line (Fig. 1d), a finding that is congruent with the higher levels of apoptosis-related DNA damage in NB4 cells (Fig. 1a, b).

Figure S1A shows that K562 cells arrest at the G1/S phase boundary and in S phase. Hence, hydroxyurea efficiently blocked its target ribonucleotide reductase and thereby the supply of dNTPs that are necessary for S phase progression. Apparently, hydroxyurea does not trigger an apoptotic replication stress response in K562 cells. To verify that hydroxyurea can evoke replicative stress and DNA damage in K562 cells, we tested for the formation of foci containing replication protein A (RPA; occur upon the accumulation of ssDNA during replicative stress) and foci containing γH2AX (Toledo et al. 2013). Immunofluorescence analyses demonstrated the formation of both types of foci in hydroxyurea-exposed K562 cells (Fig. 1e, f).

These data suggest that a loss of WT1 in hydroxyurea-treated cells indicates apoptotic cell death.

Suppression of hydroxyurea-induced apoptosis stabilizes WT1 in NB4 cells

Having assessed that a reduction of WT1 is associated with apoptosis in hydroxyurea-treated leukemic cells, we further investigated this finding. Due to the eminent role of BCL2 proteins for apoptosis induction that is linked to mitochondrial destabilization (Czabotar et al. 2014; Fulda 2015; Ni Chonghaile and Letai 2008), we tested the levels of the anti-apoptotic factors BCL-XL and BCL2 in NB4 and K562 cells. We found that K562 cells were positive for BCL-XL and expressed low levels of BCL2 (Fig. 2a). NB4 cells expressed both BCL2 proteins, but K562 cells showed much higher levels of BCL-XL than NB4 cells did (Fig. 2a). These findings are consistent with the literature (Benito et al. 1995, 1996; Delia et al. 1992; Park et al. 2003; Wu et al. 2001). In both cell lines the expression levels of BCL-XL and BCL2 were not altered by a 24 h exposure to 0.5 mM hydroxyurea (Fig. 2a).

Analyzing the expression of the pro-apoptotic factors BAX and BAK, we noted that both proteins were present at about equal levels in K562 and NB4 cells (Fig. 2b). Treatment of NB4 and K562 cells with 0.5 mM hydroxyurea for 24 or 12 h did not alter the protein levels of BAX and increased BAK levels slightly in K562 cells (Fig. 2b, Supplementary Fig. S2).

These findings suggest that the higher levels of BCL-XL protect K562 cells from apoptosis in response to hydroxyurea. To elaborate this hypothesis, we increased the levels of BCL-XL in NB4 cells and tested whether this protected NB4 cells from hydroxyurea-induced apoptosis. In addition, we overexpressed BCL2 to see whether potential effects of BCL-XL rely on this factor or are due to a general possibility to rescue NB4 cells by increased mitochondrial stability. To generate the tools for this analysis, we transduced NB4 cells with retroviruses encoding BCL2 and BCL-XL (Fig. 2c).

To confirm that cells overexpressing BCL2 and BCL-XL have an increased mitochondrial stability, we treated them and empty vector-transduced cells with hydroxyurea and measured changes in their mitochondrial membrane potentials ($\Delta\psi m$). We observed a loss of intact ψm in hydroxyurea-treated empty vector-transduced cells and that hydroxyurea-treated NB4 cells overexpressing BCL2 or BCL-XL remained their ψm nearly as intact as untreated cells (Fig. 2d). Coherent with these findings, BCL2- and BCL-XL-overexpressing NB4 cells did not activate caspase 3 fully in the presence of hydroxyurea (Fig. 2e). As expected

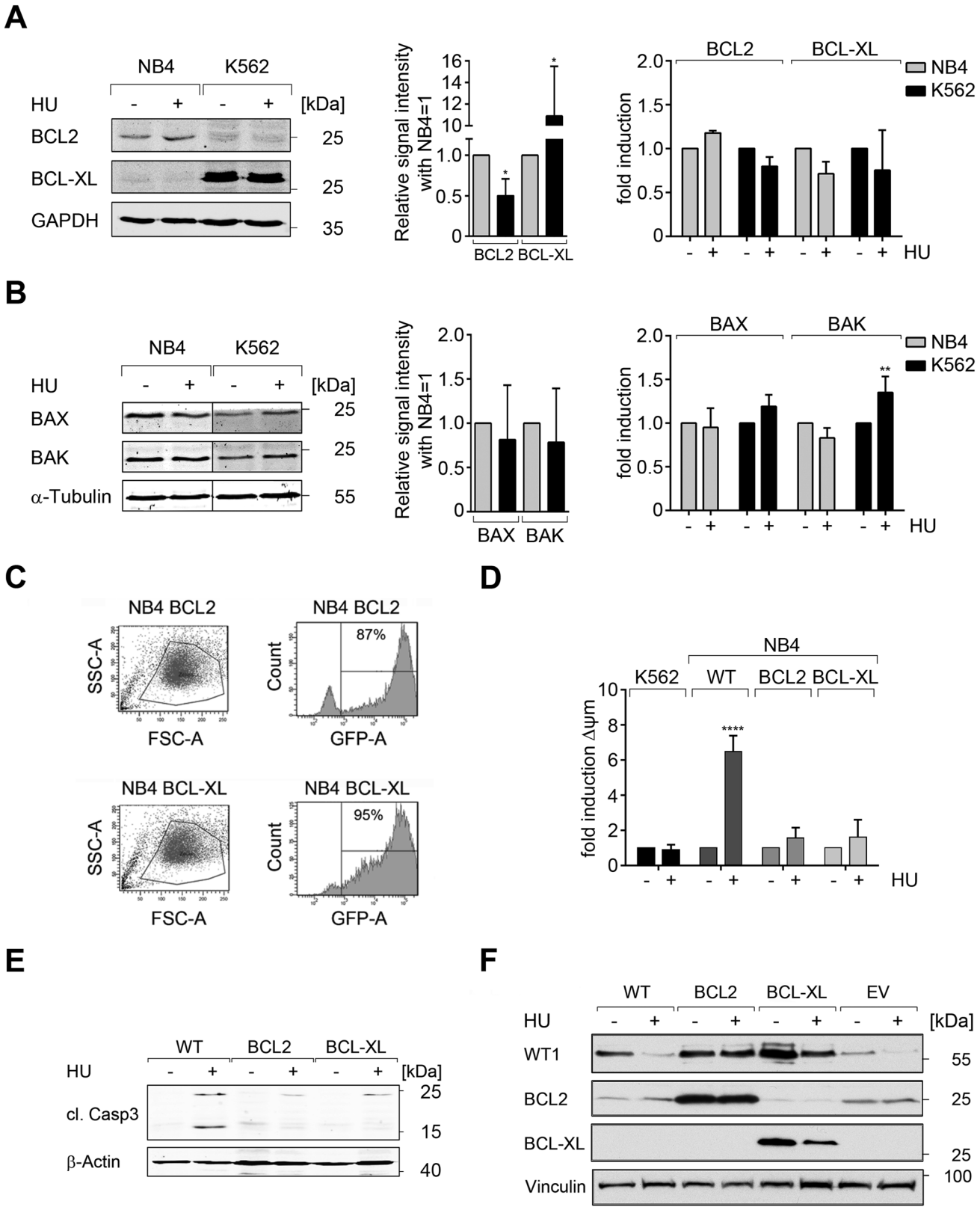

from data presented in Fig. 2a–c, ψm was unaffected by hydroxyurea in K562 cells (Fig. 2d).

Having validated our new cell systems, we tested if the overexpression of BCL2 and BCL-XL affects WT1 in hydroxyurea-treated NB4 cells. We found that wildtype

◂**Fig. 2** The mitochondrial apoptosis pathway mediates the processing of WT1. **a** Left: protein levels of BCL2 and BCL-XL in NB4 and K562 cells were analyzed by immunoblot; cells had been treated with 0.5 mM HU for 24 h; GAPDH, loading control; middle: Densitometric evaluation of BCL2 and BCL-XL levels normalized to GAPDH levels in untreated cells, NB4 is set as 1; $n = 3 \pm$ SD; unpaired, two-tailed *t* test; BCL2, $p = 0.0145$; BCL-XL, $p = 0.0203$. Right: densitometric evaluation of BCL2 and BCL-XL expression normalized to GAPDH in HU-treated cells; $n = 3 \pm$ SD. Please note: Due to the strong differences in the levels of BCL2 and BCL-XL, basal levels were set as 1 for each cell line. **b** Left: BAX and BAK levels were analyzed by immunoblot after a 24 h treatment with 0.5 mM HU; α-Tubulin, loading control; Middle: Densitometric evaluation of BAK and BAX expression normalized to α-Tubulin in untreated cells, with NB4 = 1. Right: densitometric evaluation of BAK and BAX levels in HU-treated cells normalized to α-Tubulin; $n = 4 \pm$ SD; two-way ANOVA; Bonferroni's multiple comparisons test; $^{**}p < 0.01$; basal levels of BAK and BAX in each cell line were set as 1. **c** Enrichment of EGFP-positive cells by flow cytometry after retroviral transduction of NB4 cells with a bicistronic vector containing EGFP and either BCL2 or BCL-XL. **d** Changes in the mitochondrial membrane potential ($\Delta\psi m$) were assessed by flow cytometric analysis of DiOC accumulation in the mitochondrial matrix. K562 cells, empty vector (EV, encoding only EGFP), BCL2, or BCL-XL transduced NB4 cells were treated with 0.5 mM HU for 24 h; $n = 3 \pm$ SD; two-way ANOVA; Bonferroni's multiple comparisons test; $^{****}p < 0.0001$. **e** Transduced NB4 cells were treated with 0.5 mM HU for 24 h. Immunoblot shows cleavage of caspase-3 only in HU-treated wildtype (WT) NB4 cells. **f** Immunoblot shows levels of WT1, BCL2, and BCL-XL expression in WT, BCL2, BCL-XL, or EV transduced NB4 cells treated with 0.5 mM HU for 24 h; Vinculin, loading control

NB4 cells and NB4 cells with the empty vector lost WT1. In contrast, cells overexpressing BCL2 or BCL-XL maintained higher levels of WT1 in the presence of hydroxyurea (Fig. 2f).

These results suggest that a reduced mitochondrial stability of NB4 cells leads to apoptosis and a loss of WT1 in response to hydroxyurea.

Caspases cleave WT1 in hydroxyurea-sensitive leukemic cells

As it has been reported that DNA-damaging chemotherapeutic drugs evoke the cleavage of WT1 by caspase-3 in leukemic cells (Ruan et al. 2018), we looked for such cleavage products in NB4 cells treated with 0.5 mM hydroxyurea. Western blot analyses showed that the loss of WT1 in hydroxyurea-treated NB4 cells became initiated within 6 h (Fig. 3a). This reduction of WT1 went in parallel with an early initiation of cell death (Fig. 3b).

We verified the induction of replicative stress in NB4 cells at this early time point by immunofluorescence for the presence of foci harboring RPA and γH2AX (Fig. 3c) and by Western blot for the presence of the stress-associated phosphorylated forms of RPA and H2AX (Fig. 3d).

Figure 3a further shows that hydroxyurea leads to the accumulation of WT1 species of approximately 35 kDa. To analyze if caspases catalyze such a cleavage of WT1 in NB4 cells, we treated them with hydroxyurea and the pan-caspase inhibitor z-VAD-FMK. Z-VAD-FMK efficiently rescued NB4 cells from cell death induced by hydroxyurea (Fig. 3e). This was accompanied by a lack of caspase-3 activation (Fig. 3f), which further illustrates that hydroxyurea causes apoptosis in NB4 cells. Z-VAD-FMK also attenuated the hydroxyurea-induced processing of WT1 into smaller fragments and stabilized full-length WT1 (Fig. 3g).

The remaining reduction of WT1 in NB4 cells treated with hydroxyurea and z-VAD-FMK prompted us to test with qPCR whether hydroxyurea might decrease *WT1* mRNA levels. We notice that hydroxyurea did not reduce *WT1* mRNA levels in NB4 cells (Fig. 3h).

These data suggest that the decay of WT1 is an early, apoptosis-associated event in hydroxyurea-sensitive leukemic cells.

Induction of apoptosis triggers a loss of WT1 in K562 cells

To complement our approach to protect NB4 cells from apoptosis induction by hydroxyurea, we applied pro-apoptotic conditions to K562 cells. Doxorubicin induces apoptosis and DNA damage in K562 cells (Cruet-Hennequart et al. 2012) and according to our hypothesis, doxorubicin should reduce WT1 in these cells.

Indeed, 1 µM doxorubicin induced apoptotic DNA fragmentation after 24 h (Fig. 4a) and a loss of WT1 in K562 cells (Fig. 4b). This effect was not linked to a loss of *WT1* mRNA transcripts (Fig. 3h).

Staurosporine is seen as a primarily non-genotoxic apoptosis inducer, which can kill K562 cells (Mahendrarajah et al. 2016). In those cells, staurosporine evoked a time- and dose-dependent loss of WT1, which paralleled the caspase-dependent cleavage of PARP1 (Fig. 4c).

To extend these data, we applied doxorubicin to NB4 cells. Doxorubicin induced apoptotic DNA fragmentation, the cleavage of PARP1, and a loss of WT1 (Fig. 4d, e).

Figure 4b, d, e further illustrates that hydroxyurea triggers apoptosis and WT1 processing dose-dependently in NB4 cells. K562 cells remained resistant to 1.5 mM hydroxyurea within a treatment period of 24 h (Fig. 4a).

Hence, apoptotic cell death induction with various stimuli propels a loss of the WT1 protein in leukemic cells.

The basal levels of WT1 are not predictive for the cellular sensitivity to hydroxyurea

Our data suggest that WT1 is linked to cellular survival during replicative stress. Therefore, we tested the responsiveness of a panel of leukemic cells to hydroxyurea

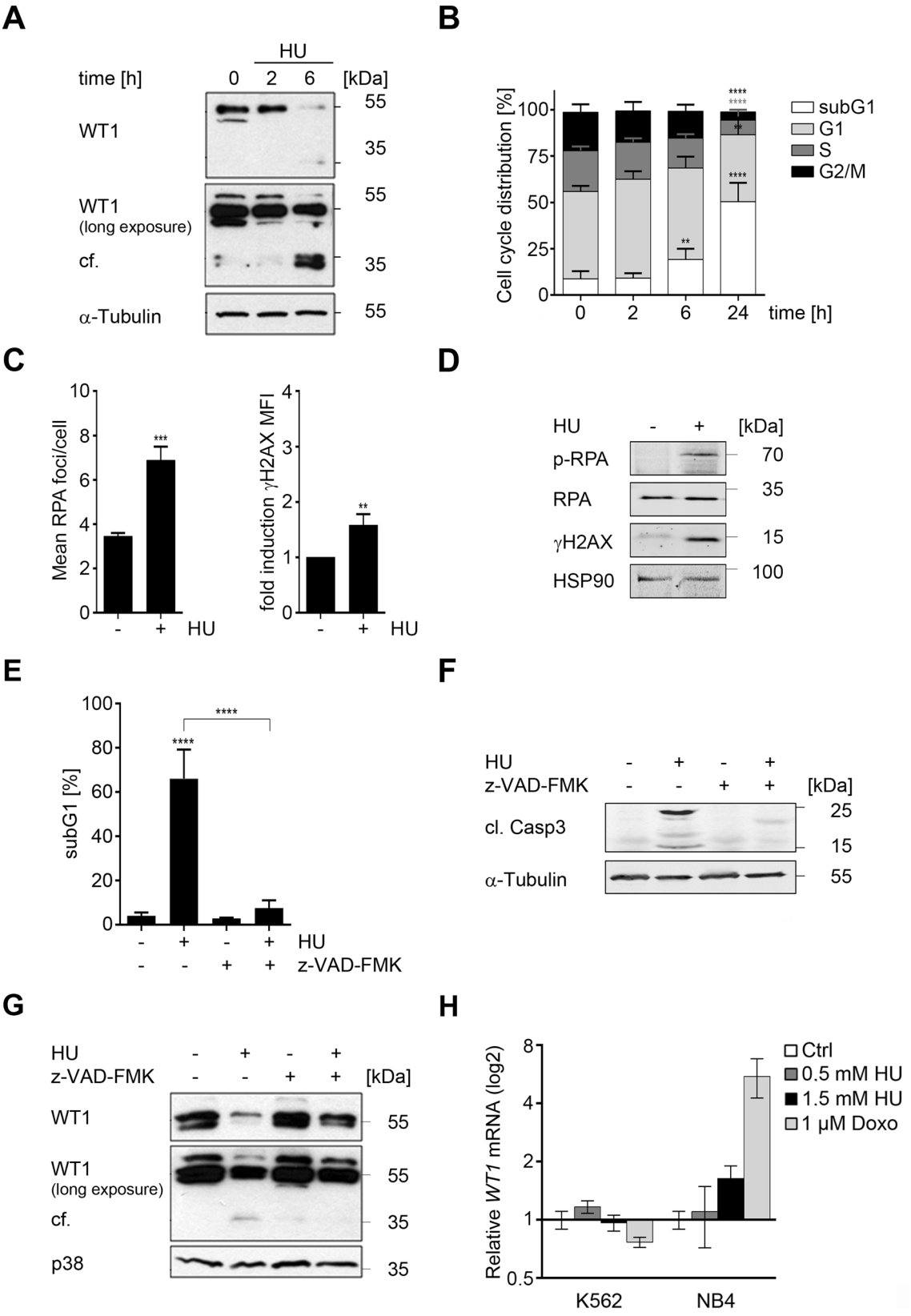
A
HU
time [h]
0
2
6
[kDa]
WT1
55
35
WT1
(long exposure)
55
cf.
35
α-Tubulin
55
B
Cell cycle distribution [%]
100
75
50
25
0
subG1
G1
S
G2/M
0
2
6
24
time [h]
C
Mean RPA foci/cell
10
8
6
4
2
0
***
- + HU
fold induction γH2AX MFI
4
3
2
1
0
**
- + HU
D
HU - +
[kDa]
p-RPA
70
RPA
35
γH2AX
15
HSP90
100
E
subG1 [%]
100
80
60
40
20
0
****
****
- + - + HU
- - + + z-VAD-FMK
F
HU - + - +
z-VAD-FMK - - + +
[kDa]
cl. Casp3
25
15
α-Tubulin
55
G
HU - + - +
z-VAD-FMK - - + +
[kDa]
WT1
55
WT1
(long exposure)
55
cf.
35
p38
35
H
Relative WT1 mRNA (log2)
8
4
2
1
0.5
Ctrl
0.5 mM HU
1.5 mM HU
1 µM Doxo
K562
NB4

◂**Fig. 3** Apoptotic caspase activation causes the cleavage of WT1 in leukemic cells. **a** Cells were treated with 0.5 mM HU for 2–6 h. Immunoblot shows WT1 expression; α-Tubulin, loading control; 0, untreated. **b** Cell cycle distribution of cells treated with 0.5 mM HU for 2–24 h; $n = 3 \pm$ SD; two-way ANOVA; Bonferroni's multiple comparisons test; $^{**}p < 0.01$, $^{****}p < 0.0001$. **c** NB4 cells were exposed to 0.5 mM HU for 6 h. RPA foci per cell were measured by immunofluorescence and quantified; $n = 3 \pm$ SD; unpaired, two-tailed Student's *t* test; $p = 0.0007$. Quantification of γH2AX mean fluorescence intensity (MFI) is shown; $n = 3 \pm$ SD; unpaired, two-tailed Student's *t* test; $p = 0.0026$. **d** NB4 cells were exposed to 0.5 mM HU for 6 h. Immunoblot shows p-T21-RPA, RPA and γH2AX; HSP90, loading control. **e** SubG1 populations of NB4 cells treated with 0.5 mM HU and/or 50 μM z-VAD-FMK for 24 h; $n = 3 \pm$ SD. one-way ANOVA; Bonferroni's multiple comparisons test; $^{****}p < 0.0001$. **f** Cells were treated as indicated for 24 h and analyzed for cleavage of caspase-3 by immunoblot; α-Tubulin, loading control. **g** Immunoblot of NB4 cells exposed to 0.5 mM HU for 24 h. WT1 expression is shown; p38, loading control. **h** *WT1* mRNA expression levels of K562 and NB4 cells treated with 0.5–1.5 mM HU or 1 μM doxorubicin (Doxo) for 24 h was measured by qPCR. *WT1* was normalized to *GAPDH* and *ACTB;* $n = 3 \pm$ SD

(Supplementary Table S1). When we analyzed eight cell lines for the expression of WT1, we found that Jurkat acute T-cell leukemia cells and U937 histiocytic leukemia cells had low to undetectable levels of *WT1* mRNA and WT1 protein expression (Fig. 5a, b).

We then tested the responses of the cells to hydroxyurea by flow cytometry assessing DNA fragmentation. Similar to WT1-positive K562 cells, WT1-negative Jurkat and U937 cells responded poorly to a 24 h exposure to 1.5 mM hydroxyurea (Fig. 5c). After a 48 h treatment with 1.5 mM hydroxyurea, K562 cells showed an increase in DNA fragmentation from 8 to 21%. This effect became more evident in U937 and Jurkat cells (from 3 to 32% and from 2 to 42%, respectively). After a 24 h treatment, the WT1-positive leukemic cells HL-60, MV4-11, RS4-11, THP-1, and NB4 showed significantly elevated DNA fragmentation. In four of these cell lines, the subG1 fractions increased up to 83–96% in response to 1.5 mM hydroxyurea applied for 48 h (Fig. 5c).

Apparently, a lack of WT1 does not sensitize leukemia cells to hydroxyurea.

Elimination of WT1 through RNAi does not cause apoptosis and does not sensitize cells to hydroxyurea

Data shown in Fig. 5 disfavor a cytoprotective role of WT1 in hydroxyurea-treated cells. However, since cell type-specific backgrounds and individual genomic lesions may override putative effects of WT1, we used siRNAs to deplete WT1 genetically in K562 cells (Fig. 6a). A transient transfection of siRNAs against the *WT1* mRNA can reduce WT1 to more than 50% after 24 h and by more than 70% after 48 h (Fig. 6a).

Having established the efficient knockdown of WT1, we treated the cells with siRNA against WT1 and with non-targeting siRNAs as control with 1 mM hydroxyurea for 24–48 h. Western blot analyses demonstrated that a knockdown of WT1 did not affect the hydroxyurea-induced phosphorylation of H2AX (Fig. 6a).

Assessing cell cycle distribution and DNA fragmentation, we noticed that K562 cells with decreased WT1 levels displayed the same cell cycle distribution as control cells. Furthermore, cells with low WT1 levels were as poorly sensitive to hydroxyurea as their WT1-positive counterparts (Fig. 6b).

To corroborate these results independently, we targeted the *WT1* mRNA with small hairpin oligonucleotides and we selected K562 cell cultures with successfully reduced WT1 levels. This attempt was efficient with various small hairpin oligonucleotides (data not shown). We chose K562 cell clones with the most efficient knockdown of WT1 for further analyses (> 80% knockdown; Fig. 6c).

Figure 6a, b further shows that an exposure of K562 cells to 1 mM hydroxyurea for 48 h attenuates WT1 levels to 49–57% of the levels in untreated cells. This process is associated with a 2.4–2.6-fold increase in cell death.

When we tested K562 with a knockout of WT1 and corresponding K562 cells that had been transfected with non-targeting shRNA control oligonucleotides, we could confirm our data collected with siRNAs against WT1. Again, the hydroxyurea-induced accumulation of γH2AX was not affected by a knockdown of WT1 (Fig. 6c). Moreover, decreasing the expression of WT1 did not alter the cell cycle or the apoptotic DNA fragmentation in response to hydroxyurea (Fig. 6d).

To complement these analyses, we isolated fresh oviduct cells from mice with an engineered *lox* cassette in front of one or both copies of the *WT1* gene (Supplementary Table S2). 4-Hydroxytamoxifen induces nuclear translocation of an estrogen receptor/Cre fusion protein (ER-Cre) and a subsequent homo-/heterozygous deletion of WT1 (Fig. 6e). Neither a heterozygous nor a homozygous deletion of WT1 affected the levels of endogenous, likely replication-associated, γH2AX foci in oviduct cells (Fig. 6e).

These data illustrate that WT1 has no obvious impact on growth, apoptosis, and DNA damage in primary oviduct cells as well as in resting and hydroxyurea-treated K562 cells.

Discussion

Our data provide several lines of evidence that stable WT1 levels are a marker for the survival of leukemic cells in the presence of hydroxyurea. Therefore, a loss of WT1 serves as surrogate marker predicting the sensitivity of leukemic

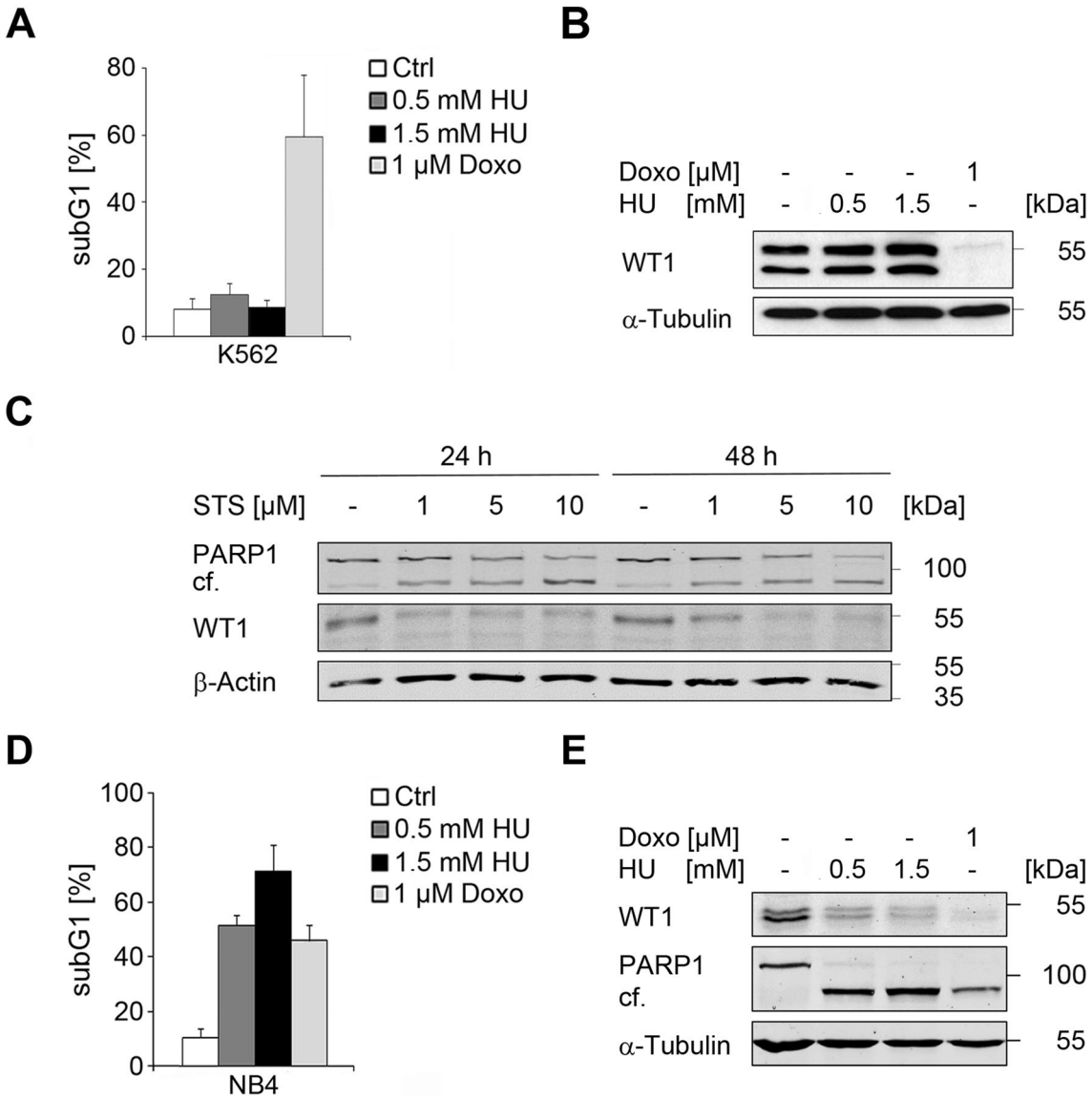

Fig. 4 Doxorubicin and staurosporine cause apoptosis and a loss of WT1. **a** SubG1 populations of K562 cells treated with 0.5–1.5 mM HU or 1 µM Doxo for 24 h; $n = 3 \pm$ SD. **b** Aliquots of these cells were analyzed for WT1 expression by immunoblot; α-Tubulin, loading control. **c** Immunoblot shows PARP1 and WT1 expression in K562 cells treated with 1–10 µM staurosporine (STS) for 24–48 h; β-Actin, loading control; cf., cleaved fragment. **d** NB4 cells treated with 0.5 mM, 1.5 mM HU or 1 µM Doxo for 24 h were used to determine the occurrence of subG1 fractions; $n = 3 \pm$ SD. **e** Aliquots of these cells were analyzed for WT1 expression and PARP1 cleavage by immunoblot; α-Tubulin, loading control

cells to hydroxyurea (Fig. 7). Pro-apoptotic conditions that are induced by doxorubicin and staurosporine can target hydroxyurea-resistant cells and this is associated with a loss of WT1. Similar observations are mirrored in clinical studies, which report that residual WT1 expression indicates treatment failures and high relapse rates of AML and CML patients under chemotherapy (Ariyaratana and Loeb 2007; Hastie 2017; Huff 2011; Rampal and Figueroa 2016).

We confirm the processing of WT1 by caspases, which leads to the occurrence of new WT1 cleavage products at around 35 kDa (Ruan et al. 2018). These are different from the 20 kDa cleavage product generated by the serine protease HTRA2/OMI (Hartkamp et al. 2010). We noted that z-VAD-FMK could not restore WT1 fully in NB4 cells exposed to hydroxyurea. This may stem from the processing of WT1 by HTRA2 (Hartkamp et al. 2010).

As the anti-WT1 C19 antibody we used recognizes a C-terminal epitope of WT1 (Hartkamp et al. 2010), we conclude that the 35 kDa cleavage products contain the C-terminal, DNA-binding part of WT1. Although one may postulate pro-apoptotic effects of WT1 fragments, transfection of such

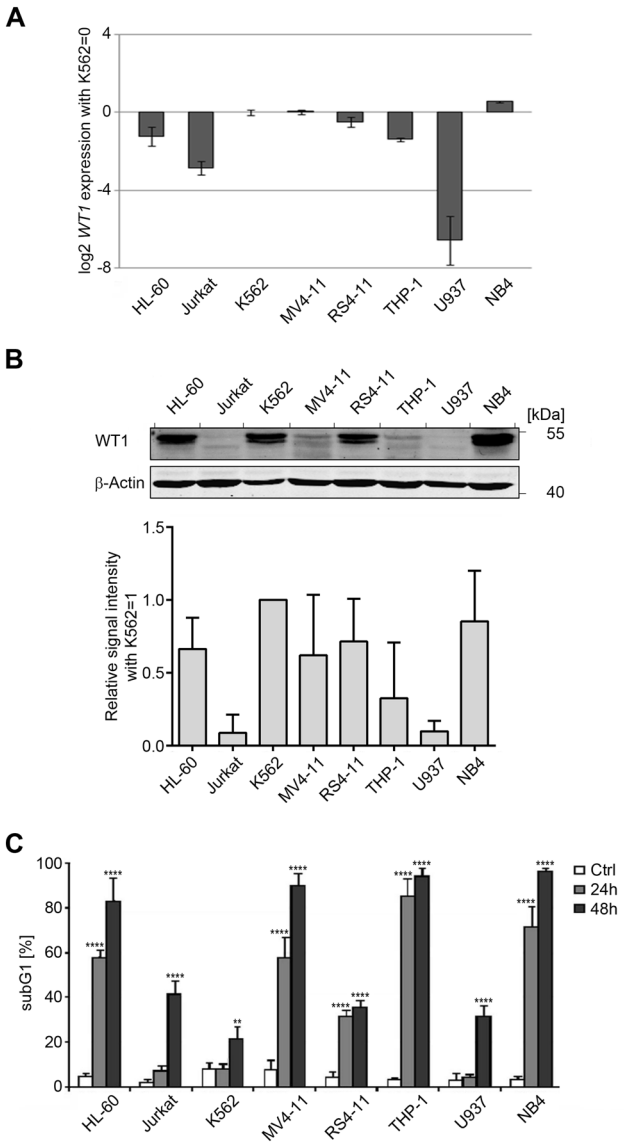

Fig. 5 Expression of WT1 in different leukemic cell lines and apoptosis induction in response to hydroxyurea. **a** Expression of *WT1* mRNA levels was determined by quantitative real-time PCR in various leukemic cell lines with the expression level of K562 = 1, $n = 3 \pm$ SD. WT1 expression was normalized to *ACTB, GAPDH, HPRT* and *TBP*. **b** WT1 expression on protein level was detected via immunoblot. Densitometric analysis of WT1 with K562 = 1; $n = 3 \pm$ SD. Initial results were normalized to LDH; LDH, loading control. **c** Cells were treated with 1.5 mM HU for 24–48 h. SubG1 numbers were determined by cell cycle analysis of PI-stained, fixed cells via flow cytometry; $n = 3$–$4 \pm$ SD; two-way ANOVA; Bonferroni's multiple comparisons test; $^{**}p < 0.01$, $^{****}p < 0.0001$

fragments does not cause apoptosis (Hartkamp et al. manuscript in preparation).

Despite our evidence on a correlation between the decrease in WT1 and cell death, our loss-of-function approaches illustrate that a genetic reduction of WT1 by RNAi cannot augment the sensitivity of K562 cells towards hydroxyurea-induced apoptosis and DNA damage. Thus, although WT1 is seen as a promising target for cytotoxic cancer therapy, our data suggest that WT1 represents a target of caspases but not an upstream regulator of chemotherapy-induced cell death. At first glance, such data are in contrast to other reports stating a positive survival effect of WT1 on stressed leukemic cells (Bansal et al. 2010; Ito et al. 2006; Li et al. 2014; Ruan et al. 2018). Nonetheless, others have also questioned whether the levels of WT1 are important for the survival of K562 cells treated with the DNA-damaging agent etoposide (Svensson et al. 2007) and earlier reports found that an overexpression of WT1 isoforms cannot protect K562 cells from the genotoxic drugs cis-platin and doxorubicin (Carrington and Algar 2000). It has been speculated (Svensson et al. 2007) that a reduced sensitivity of K562 cells overexpressing the 17AA(+)KTS(−) isoform of WT1 (Ito et al. 2006) is due to a selection of a K562 cell clone. Furthermore, it has to be considered that WT1 is a caspase target [(Ruan et al. 2018) and this work] and its overexpression (Ito et al. 2006) may buffer caspase activity. Such effects have been seen with other proteins and in other cellular systems under replicative stress (e.g., Krämer et al. 2008) and may explain the correlation between WT1 and drug resistance.

Our work additionally informs about the functions of WT1 in resting cells. While others found that WT1 ensures the growth and survival of K562 cells (Ito et al. 2006; Renshaw et al. 2004), we and others could not confirm this notion (Bansal et al. 2010, and this work). Despite a knockdown of up to 80% of WT1 at the protein level, we do not see that a genetic elimination of WT1 in K562 cells has adverse effects on their growth and vitality. Although different culture conditions may be a reason for such discrepancies, we believe that our findings correspond well with the observation that several cancer cells express no detectable WT1, but grow and survive well. Moreover, HL-60 and KG-1 leukemic cells even grow faster when WT1 is eliminated (Wang et al. 2015).

Mutations in WT1 may also regulate the sensitivity of leukemic cells to hydroxyurea, as such mutations correlate with chemoresistance (Ariyaratana and Loeb 2007; Hastie 2017; Huff 2011; Rampal and Figueroa 2016). Such mutations often lead to a loss-of-function of WT1 (Ariyaratana and Loeb 2007; Hastie 2017; Huff 2011; Rampal and Figueroa 2016) and altered DNA methylation patterns (Rampal et al. 2014; Wang et al. 2015). As hydroxyurea has a certain effect on methylation patterns (Pule et al. 2015), a loss of WT1 may affect cellular reactions to this drug.

It may appear surprising that we see no adverse effect of a WT1 reduction on cell proliferation, as WT1 controls mitosis together with the protein MAD2 in kidney-derived cells (Shandilya et al. 2014). However, the different results are likely due to cell type-specific components, as WT1 also

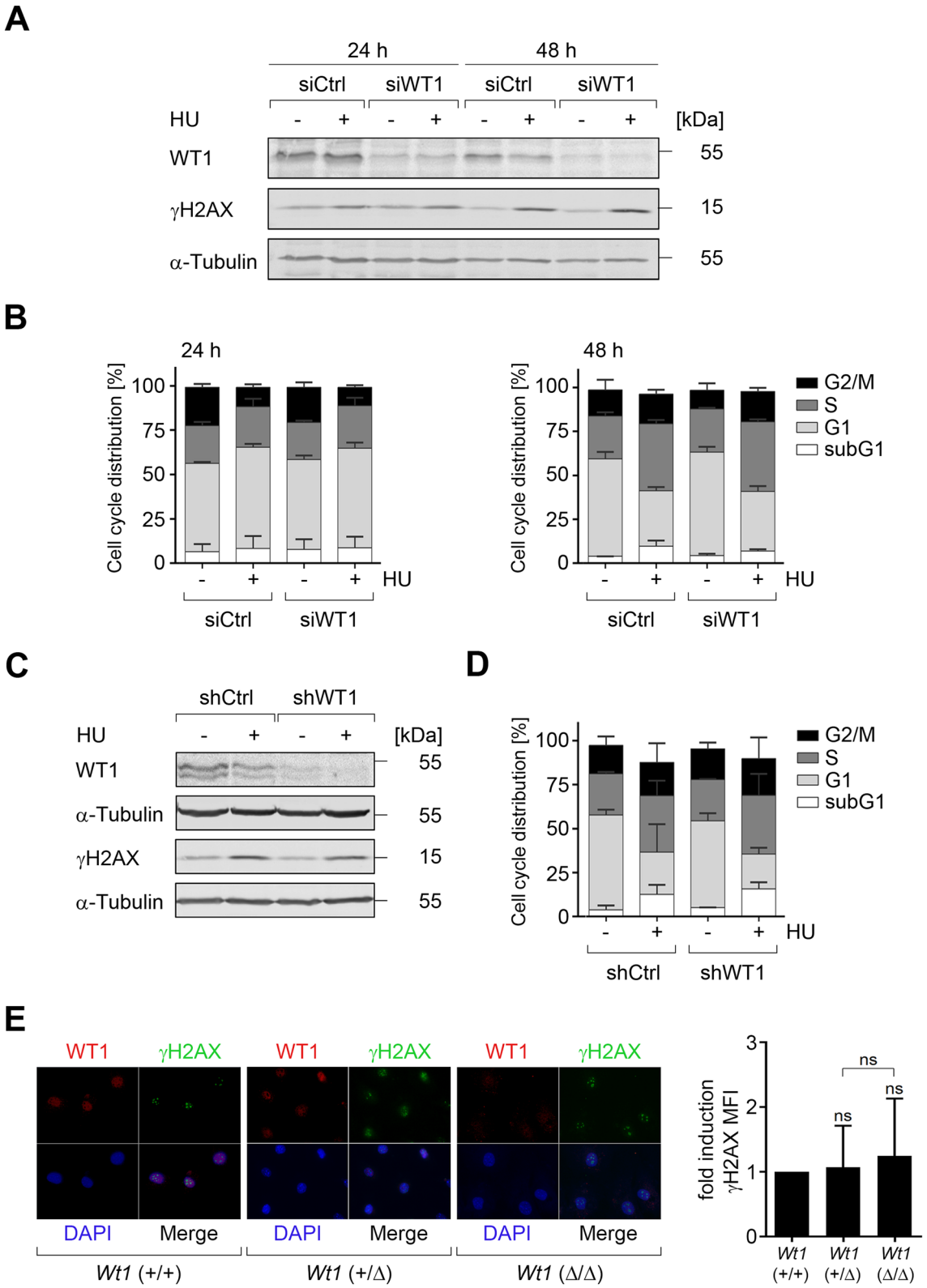
A
24 h
48 h
siCtrl
siWT1
siCtrl
siWT1
HU
- + - + - + - +
[kDa]
WT1
55
γH2AX
15
α-Tubulin
55
B
24 h
48 h
Cell cycle distribution [%]
100
75
50
25
0
G2/M
S
G1
subG1
HU
siCtrl
siWT1
C
shCtrl
shWT1
HU
- + - +
[kDa]
WT1
55
α-Tubulin
55
γH2AX
15
α-Tubulin
55
D
Cell cycle distribution [%]
shCtrl
shWT1
E
WT1
γH2AX
DAPI
Merge
Wt1 (+/+)
Wt1 (+/Δ)
Wt1 (Δ/Δ)
fold induction γH2AX MFI
ns
3
2
1
0
Wt1 (+/+)
Wt1 (+/Δ)
Wt1 (Δ/Δ)

◂**Fig. 6** Knockdown of WT1 has no effect on cell cycle or apoptosis. **a** Knockdown of WT1 in K562 cells with RNAi. Following transfection, cells were treated with 1 mM HU for 24–48 h and analyzed for expression of WT1 and γH2AX by immunoblot; α-Tubulin, loading control. **b** For cell cycle distribution PI-stained, fixed cells were measured via flow cytometry; $n=3\pm$SD. **c** K562 shCtrl and shWT1 cells treated with 1 mM HU for 48 h were analyzed for WT1, and γH2AX expression by immunoblot; α-Tubulin, loading control. **d** Cell cycle distributions of PI-stained, fixed cells are shown; $n=3\pm$SD. **e** *Wt1* wildtype (+/+), *Wt1* heterozygous (+/Δ) and *Wt1* knockout (Δ/Δ) primary oviduct cells were analyzed for WT1 expression (red) and γH2AX (green) by immunofluorescence. Nuclei were stained with DAPI (blue). The fold induction of γH2AX mean fluorescence intensity (MFI) was measured with imageJ. For the quantification a total cell number of (+/+)=23, (+/Δ)=70, (Δ/Δ)=55 was used; one-way ANOVA; *ns* not significant. (Color figure online)

exerts no effects on the mitotic checkpoint in MCF7 breast cancer cells (Shandilya et al. 2014). It should additionally be considered that hydroxyurea inhibits the cellular dNTP supply to prevent the entry of cells into the G2/M phase, where the WT1/MAD2 interplay operates.

Whether leukemic cells lose or keep WT1 in response to hydroxyurea does not affect the expression of pro- and anti-apoptotic BCL2 family members (BCL-XL, BCL2, BAX, BAK) in our analyzed cell systems. While these findings contradict other reports (Bansal et al. 2010, 2012; Ito et al. 2006), a lack of correlation between WT1 levels and BAX and BCL2 was similarly observed in murine 32D leukemia cells, in which WT1 17AA(−)KTS(−) regulates the anti-apoptotic BCL2 member A1/BFL-1 (Simpson et al. 2006). The concomitant reduction of BCL2 and WT1 in the presence of an HSP90 inhibitor (Bansal et al. 2010, 2012) might be a consequence of additional effects.

We demonstrate that BCL-XL is expressed at much higher levels in cells that do not undergo apoptosis in response to hydroxyurea (Fig. 7) and that overexpressed BCL-XL can rescue hydroxyurea-sensitive cells. Curiously, this observation is not restricted to a certain BCL2 family member, but protective effects can equally be achieved with an overexpression of BCL2. Such a finding is consistent with the possibility to stabilize mitochondrial membranes by both BCL-XL and BCL2 (Czabotar et al. 2014; Fulda 2015; Loeb 2006; Ni Chonghaile and Letai 2008).

Truly, other signaling pathways may also control the sensitivity of leukemic cells to hydroxyurea. For example, BCR-ABL positive K562 cells show a strong activation of the survival factor STAT5, which could protect against hydroxyurea. However, p-STAT5 does not correlate with the resistance of BCR-ABL-positive cells to hydroxyurea (Warsch et al. 2011). Another candidate is the tumor suppressor p53, which is often lost and mutated in cancer cells (Schneider and Krämer 2011). Yet, there is no obvious correlation between the p53 status and the sensitivity of leukemic

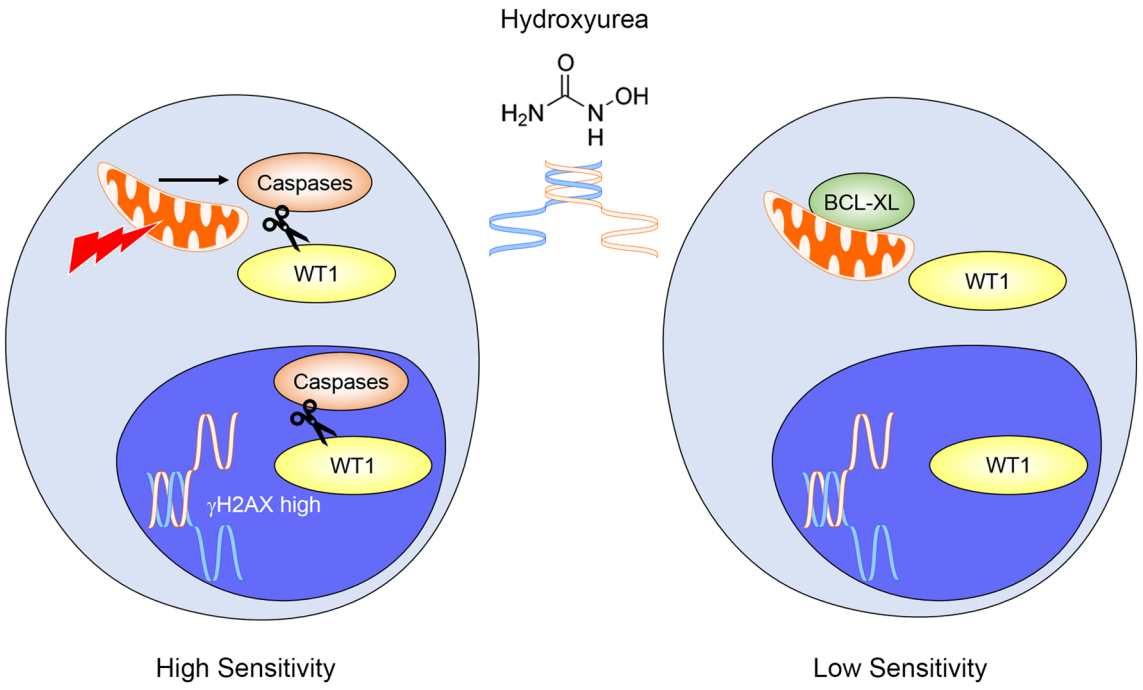

Fig. 7 Model: Response to hydroxyurea. Caspases cleave WT1 in cells that are highly sensitive to HU. Less sensitive cells are protected by anti-apoptotic BCL-XL

cells to hydroxyurea (Supplementary Table S1). Further studies are underway to decipher molecular mechanisms of hydroxyurea resistance and sensitivity and how these might be exploited therapeutically.

Taken together, a caspase-dependent processing of WT1 is a marker for hydroxyurea-induced apoptosis via the mitochondrial pathway. Thus, WT1 might be of diagnostic and predictive value for the chemotherapy of leukemic disorders.

Acknowledgements We thank Christina Brachetti and Birgit Rasenberger (Department of Toxicology, UM Mainz, Germany), and Christiane Becker (UKE Aachen, Germany) for excellent technical support, and Richard Moriggl, Medical University Vienna, for BCL2/BCL-XL expression constructs. Gesine Bug (University Clinic Frankfurt/Main, Germany) and all members of the Department of Toxicology, UM Mainz were excellent discussion partners. Grant support: German Cancer Aid (#110909 and #110125 to OHK, and #109528 to CS/CE), Wilhelm Sander Foundation (#2010.078.2 to OHK), and Deutsche Forschungsgemeinschaft (#KR2291/5-1 and KR2291/7-1 to OHK).

Compliance with ethical standards

Conflict of interest The authors declare no conflict of interest.

References

Ariyaratana S, Loeb DM (2007) The role of the Wilms tumour gene (WT1) in normal and malignant haematopoiesis. Expert Rev Mol Med 9(14):1–17. https://doi.org/10.1017/S1462399407000336

Bansal H, Bansal S, Rao M et al (2010) Heat shock protein 90 regulates the expression of Wilms tumor 1 protein in myeloid leukemias. Blood 116(22):4591–4599. https://doi.org/10.1182/blood-2009-10-247239

Bansal H, Seifert T, Bachier C et al (2012) The transcription factor Wilms tumor 1 confers resistance in myeloid leukemia cells against the proapoptotic therapeutic agent TRAIL (tumor necrosis factor alpha-related apoptosis-inducing ligand) by regulating the antiapoptotic protein Bcl-xL. J Biol Chem 287(39):32875–32880. https://doi.org/10.1074/jbc.C112.366559

Benito A, Grillot D, Nunez G, Fernandez-Luna JL (1995) Regulation and function of Bcl-2 during differentiation-induced cell death in HL-60 promyelocytic cells. Am J Pathol 146(2):481–490

Benito A, Silva M, Grillot D, Nunez G, Fernandez-Luna JL (1996) Apoptosis induced by erythroid differentiation of human leukemia cell lines is inhibited by Bcl-XL. Blood 87(9):3837–3843

Bergmann L, Miething C, Maurer U et al (1997) High levels of Wilms' tumor gene (wt1) mRNA in acute myeloid leukemias are associated with a worse long-term outcome. Blood 90(3):1217–1225

Beyer M, Kiweler N, Mahboobi S, Krämer OH (2017) How to distinguish between the activity of HDAC1-3 and HDAC6 with western blot. Methods Mol Biol 1510:355–364. https://doi.org/10.1007/978-1-4939-6527-4_26

Bongso A, Ng SC, Sathananthan H, Ng PL, Rauff M, Ratnam SS (1989) Establishment of human ampullary cell cultures. Hum Reprod 4(5):486–494

Bourkoula K, Englert C, Giaisi M, Kohler R, Krammer PH, Li-Weber M (2014) The Wilms' tumor suppressor WT1 enhances CD95L expression and promotes activation-induced cell death in leukemic T cells. Int J Cancer 134(2):291–300. https://doi.org/10.1002/ijc.28379

Buchwald M, Pietschmann K, Müller JP, Böhmer FD, Heinzel T, Krämer OH (2010) Ubiquitin conjugase UBCH8 targets active FMS-like tyrosine kinase 3 for proteasomal degradation. Leukemia 24(8):1412–1421. https://doi.org/10.1038/leu.2010.114

Carrington D, Algar E (2000) Overexpression of murine WT1 +/+ and −/− isoforms has no effect on chemoresistance but delays differentiation in the K562 leukemia cell line. Leuk Res 24(11):927–936

Cruet-Hennequart S, Prendergast AM, Shaw G, Barry FP, Carty MP (2012) Doxorubicin induces the DNA damage response in cultured human mesenchymal stem cells. Int J Hematol 96(5):649–656. https://doi.org/10.1007/s12185-012-1196-5

Czabotar PE, Lessene G, Strasser A, Adams JM (2014) Control of apoptosis by the BCL-2 protein family: implications for physiology and therapy. Nat Rev Mol Cell Biol 15(1):49–63. https://doi.org/10.1038/nrm3722

Delia D, Aiello A, Soligo D et al (1992) bcl-2 proto-oncogene expression in normal and neoplastic human myeloid cells. Blood 79(5):1291–1298

Dobbelstein M, Sørensen CS (2015) Exploiting replicative stress to treat cancer. Nat Rev Drug Discov 14(6):405–423. https://doi.org/10.1038/nrd4553

Ellisen LW, Carlesso N, Cheng T, Scadden DT, Haber DA (2001) The Wilms tumor suppressor WT1 directs stage-specific quiescence and differentiation of human hematopoietic progenitor cells. EMBO J 20(8):1897–1909. https://doi.org/10.1093/emboj/20.8.1897

Fulda S (2015) Targeting extrinsic apoptosis in cancer: challenges and opportunities. Semin Cell Dev Biol 39:20–25. https://doi.org/10.1016/j.semcdb.2015.01.006

Gianfaldoni G, Mannelli F, Ponziani V et al (2010) Early reduction of WT1 transcripts during induction chemotherapy predicts for longer disease free and overall survival in acute myeloid leukemia. Haematologica 95(5):833–836. https://doi.org/10.3324/haematol.2009.011908

Gray JX, McMillen L, Mollee P et al (2012) WT1 expression as a marker of minimal residual disease predicts outcome in acute myeloid leukemia when measured post-consolidation. Leuk Res 36(4):453–458. https://doi.org/10.1016/j.leukres.2011.09.005

Grimwade D, Vyas P, Freeman S (2010) Assessment of minimal residual disease in acute myeloid leukemia. Curr Opin Oncol 22(6):656–663. https://doi.org/10.1097/CCO.0b013e32833ed831

Hartkamp J, Carpenter B, Roberts SG (2010) The Wilms' tumor suppressor protein WT1 is processed by the serine protease HtrA2/Omi. Mol Cell 37(2):159–171. https://doi.org/10.1016/j.molcel.2009.12.023

Hastie ND (2017) Wilms' tumour 1 (WT1) in development, homeostasis and disease. Development 144(16):2862–2872. https://doi.org/10.1242/dev.153163

Hosen N, Shirakata T, Nishida S et al (2007) The Wilms' tumor gene WT1-GFP knock-in mouse reveals the dynamic regulation of WT1 expression in normal and leukemic hematopoiesis. Leukemia 21(8):1783–1791. https://doi.org/10.1038/sj.leu.2404752

Huff V (2011) Wilms' tumours: about tumour suppressor genes, an oncogene and a chameleon gene. Nat Rev Cancer 11(2):111–121. https://doi.org/10.1038/nrc3002

Ito K, Oji Y, Tatsumi N et al (2006) Antiapoptotic function of 17AA(+) WT1 (Wilms' tumor gene) isoforms on the intrinsic apoptosis pathway. Oncogene 25(30):4217–4229. https://doi.org/10.1038/sj.onc.1209455

Itzykson R, Fenaux P, Solary E (2013) Chronic myelomonocytic leukemia: myelodysplastic or myeloproliferative? Best practice research. Clin Haematol 26(4):387–400. https://doi.org/10.1016/j.beha.2013.09.006

Krämer OH, Knauer SK, Zimmermann D, Stauber RH, Heinzel T (2008) Histone deacetylase inhibitors and hydroxyurea modulate the cell cycle and cooperatively induce apoptosis. Oncogene 27(6):732–740. https://doi.org/10.1038/sj.onc.1210677

Kühnl A, Kaiser M, Neumann M et al (2011) High expression of IGFBP2 is associated with chemoresistance in adult acute myeloid leukemia. Leuk Res 35(12):1585–1590. https://doi.org/10.1016/j.leukres.2011.08.006

Lapillonne H, Renneville A, Auvrignon A et al (2006) High WT1 expression after induction therapy predicts high risk of relapse and death in pediatric acute myeloid leukemia. J Clin Oncol 24(10):1507–1515. https://doi.org/10.1200/JCO.2005.03.5303

Li X, Li Y, Yuan T et al (2014) Exogenous expression of WT1 gene influences U937 cell biological behaviors and activates MAPK and JAK-STAT signaling pathways. Leukemia Res 38(8):931–939. https://doi.org/10.1016/j.leukres.2014.05.006

Loeb DM (2006) WT1 influences apoptosis through transcriptional regulation of Bcl-2 family members. Cell Cycle 5(12):1249–1253. https://doi.org/10.4161/cc.5.12.2807

Lyu Y, Lou J, Yang Y et al (2017) Dysfunction of the WT1-MEG3 signaling promotes AML leukemogenesis via p53-dependent and -independent pathways. Leukemia. https://doi.org/10.1038/leu.2017.116

Madaan K, Kaushik D, Verma T (2012) Hydroxyurea: a key player in cancer chemotherapy. Expert Rev Anticancer Ther 12(1):19–29. https://doi.org/10.1586/era.11.175

Mahendrarajah N, Paulus R, Krämer OH (2016) Histone deacetylase inhibitors induce proteolysis of activated CDC42-associated kinase-1 in leukemic cells. J Cancer Res Clin Oncol 142(11):2263–2273. https://doi.org/10.1007/s00432-016-2229-x

Makki MS, Heinzel T, Englert C (2008) TSA downregulates Wilms tumor gene 1 (Wt1) expression at multiple levels. Nucleic Acids Res 36(12):4067–4078. https://doi.org/10.1093/nar/gkn356

Marx-Blümel L, Marx C, Kühne M, Sonnemann J (2017) Assessment of HDACi-Induced Cytotoxicity. Methods Mol Biol 1510:23–45. https://doi.org/10.1007/978-1-4939-6527-4_3

Miglino M, Colombo N, Pica G et al (2011) WT1 overexpression at diagnosis may predict favorable outcome in patients with de novo non-M3 acute myeloid leukemia. Leuk Lymphoma 52(10):1961–1969. https://doi.org/10.3109/10428194.2011.585673

Montano G, Cesaro E, Fattore L et al (2013) Role of WT1-ZNF224 interaction in the expression of apoptosis-regulating genes. Hum Mol Genet 22(9):1771–1782. https://doi.org/10.1093/hmg/ddt027

Montano G, Vidovic K, Palladino C et al (2015) WT1-mediated repression of the proapoptotic transcription factor ZNF224 is triggered by the BCR-ABL oncogene. Oncotarget 6(29):28223–28237. https://doi.org/10.18632/oncotarget.4950

Ni Chonghaile T, Letai A (2008) Mimicking the BH3 domain to kill cancer cells. Oncogene 27 Suppl 1:S149–S157 https://doi.org/10.1038/onc.2009.52

Nikolova T, Kiweler N, Krämer OH (2017) Interstrand crosslink repair as a target for HDAC inhibition. Trends Pharmacol Sci. https://doi.org/10.1016/j.tips.2017.05.009

Park DJ, Vuong PT, de Vos S, Douer D, Koeffler HP (2003) Comparative analysis of genes regulated by PML/RAR alpha and PLZF/RAR alpha in response to retinoic acid using oligonucleotide arrays. Blood 102(10):3727–3736. https://doi.org/10.1182/blood-2003-02-0412

Pfaffl MW, Horgan GW, Dempfle L (2002) Relative expression software tool (REST) for group-wise comparison and statistical analysis of relative expression results in real-time PCR. Nucleic Acids Res 30(9):e36

Pule GD, Mowla S, Novitzky N, Wiysonge CS, Wonkam A (2015) A systematic review of known mechanisms of hydroxyurea-induced fetal hemoglobin for treatment of sickle cell disease. Expert Rev Hematol 8(5):669–679. https://doi.org/10.1586/17474086.2015.1078235

Rampal R, Figueroa ME (2016) Wilms tumor 1 mutations in the pathogenesis of acute myeloid leukemia. Haematologica 101(6):672–679. https://doi.org/10.3324/haematol.2015.141796

Rampal R, Alkalin A, Madzo J et al (2014) DNA hydroxymethylation profiling reveals that WT1 mutations result in loss of TET2 function in acute myeloid leukemia. Cell Rep 9(5):1841–1855. https://doi.org/10.1016/j.celrep.2014.11.004

Renshaw J, Orr RM, Walton MI et al (2004) Disruption of WT1 gene expression and exon 5 splicing following cytotoxic drug treatment: antisense down-regulation of exon 5 alters target gene expression and inhibits cell survival. Mol Cancer Therap 3(11):1467–1484

Rogakou EP, Pilch DR, Orr AH, Ivanova VS, Bonner WM (1998) DNA double-stranded breaks induce histone H2AX phosphorylation on serine 139. J Biol Chem 273(10):5858–5868

Ruan J, Gao S, Yang J, Li H, Huang H, Zheng X (2018) WT1 protein is cleaved by caspase-3 in apoptotic leukemic cells. Leuk Lymphoma 59(1):162–170. https://doi.org/10.1080/10428194.2017.1312368

Schlacher K, Christ N, Siaud N, Egashira A, Wu H, Jasin M (2011) Double-strand break repair-independent role for BRCA2 in blocking stalled replication fork degradation by MRE11. Cell 145(4):529–542. https://doi.org/10.1016/j.cell.2011.03.041

Schneider G, Krämer OH (2011) NFkappaB/p53 crosstalk—a promising new therapeutic target. Biochim Biophys Acta 1815(1):90–103. https://doi.org/10.1016/j.bbcan.2010.10.003

Shandilya J, Toska E, Richard DJ, Medler KF, Roberts SG (2014) WT1 interacts with MAD2 and regulates mitotic checkpoint function. Nat Commun 5:4903. https://doi.org/10.1038/ncomms5903

Simpson LA, Burwell EA, Thompson KA, Shahnaz S, Chen AR, Loeb DM (2006) The antiapoptotic gene A1/BFL1 is a WT1 target gene that mediates granulocytic differentiation and resistance to chemotherapy. Blood 107(12):4695–4702. https://doi.org/10.1182/blood-2005-10-4025

Svensson E, Vidovic K, Lassen C et al (2007) Deregulation of the Wilms' tumour gene 1 protein (WT1) by BCR/ABL1 mediates resistance to imatinib in human leukaemia cells. Leukemia 21(12):2485–2494. https://doi.org/10.1038/sj.leu.2404924

Toledo LI, Altmeyer M, Rask MB et al (2013) ATR prohibits replication catastrophe by preventing global exhaustion of RPA. Cell 155(5):1088–1103. https://doi.org/10.1016/j.cell.2013.10.043

Treude F, Kappes F, Fahrenkamp D et al (2014) Caspase-8-mediated PAR-4 cleavage is required for TNFalpha-induced apoptosis. Oncotarget 5(10):2988–2998. https://doi.org/10.18632/oncotarget.1634

Varma N, Anand MS, Varma S, Juneja SS (2011) Role of hTERT and WT1 gene expression in disease progression and imatinib responsiveness of patients with BCR-ABL positive chronic myeloid leukemia. Leuk Lymphoma 52(4):687–693. https://doi.org/10.3109/10428194.2010.550978

Wang Y, Xiao M, Chen X et al (2015) WT1 recruits TET2 to regulate its target gene expression and suppress leukemia cell proliferation. Mol Cell 57(4):662–673. https://doi.org/10.1016/j.molcel.2014.12.023

Warsch W, Kollmann K, Eckelhart E et al (2011) High STAT5 levels mediate imatinib resistance and indicate disease progression in chronic myeloid leukemia. Blood 117(12):3409–3420. https://doi.org/10.1182/blood-2009-10-248211

Wu Y, Mehew JW, Heckman CA, Arcinas M, Boxer LM (2001) Negative regulation of bcl-2 expression by p53 in hematopoietic cells. Oncogene 20(2):240–251. https://doi.org/10.1038/sj.onc.1204067